Effect of the soil on the metal detector signature of a buried mine

Pascal Druyts[a], Yogadhish Das[b], Christophe Craeye[c] and Marc Acheroy[a]

[a] RMA, Signal and Image Centre, Av. de la Renaissance 30, 1000 Brussels, Belgium.
[b] Defence R&D Canada, Suffield, Alberta, Canada.
[c] UCL, ELTM department, Place du Levant 3, B-1348 Louvain-la-Neuve, Belgium.

ABSTRACT

This paper analyzes the effect of the soil on the response of a metal detector (MD). The total response is first decomposed in a direct coupling between the transmitter and the receiver, the mine contribution and the soil contribution. The mine contribution is further related to its free space signature by introducting a number of transfer functions (TFs). Those TFs characterize the effect of the soil on the field propagation, from the transmit coil to the mine and back to the receiver, and on the mine signature. The expressions derived are quite general. However the TFs and other quantities of interest can only be computed if the scattering problem has been solved. For this it is usually necessary to resort to numerical techniques. Such techniques are computationally expensive, especially to analyze the various effects of the soil as they require to compute the solution for a large set of parameters. Therefore, we propose to model a buried mine by a multilayered sphere. From outside to inside, the layers represent the air, the soil, the mine explosive and the mine metallic content. Further, the analytic solution for such a multilayered sphere is used to compute the mine and soil responses, the mine free space signature and the various TFs as a function of the parameters of interest such as the soil electromagnetic (EM) properties or the mine depth. Finally, the validity domain of a number of practical approximations is discussed.

Keywords: metal detector, humanitarian demining, mine signature, soil compensation, multipole expansion, reciprocity, layered sphere

1. INTRODUCTION

The signal measured by a MD swept over a buried mine in general includes a soil and a target contribution. For adverse soils, the soil contribution can dominate the mine signal. Therefore, to reduce the number of false alarms generated by the soil, high-end detectors use soil compensation techniques which play an important role from an operational point of view. Those compensation technique use differences that may exist between the mine and the soil response to cancel the soil response without significantly reducing the mine response.

To assess the soil influence on the detection capability of a MD and the efficiency of the various soil compensation techniques, it is crucial to understand the soil effect on the MD response. The analysis of this effect is in general quite complex as the soil not only generates an additional signal but also influences the field propagation from the transmit coil to the target and back to the receive coil and affects on the target signature itself.

To analyze those effects, a number of approximations are classically made in the literature. First, if the target is assumed small enough, it can be modeled by its magnetic polarizability tensor [1, p. 23]. The underlying assumption being that the incident field is homogeneous on the target and that the scattered field, as seen by the receiver, can be accurately approximated by the field of a magnetic dipole. Secondly, if the soil is assumed weakly reactive—$\mu \backsimeq \mu_0$, $\sigma \backsimeq 0$—, the magnetic polarizability tensor is assumed to be identical to its free space counterpart [1, p. 170] or to what it would be in a full space filled with soil [2,3]. Similarly, the effect of the soil on the field transmission is either taken into account [2,3] or not [1, p. 170].

From actual values of soil parameters [4, p. 53][5] it appears that soils are indeed weakly reactive. Therefore the question arises why soil compensation is a challenge for MD manufacturers. It turns out that the mine metal

Send correspondence to Pascal Druyts
E-mail: Pascal.Druyts@elec.rma.ac.be , Telephone: 32 2 737 6665

Detection and Remediation Technologies for Mines and Minelike Targets XI, edited by J. Thomas Broach, Russell S. Harmon, John H. Holloway, Proc. of SPIE Vol. 6217, 62170Q, (2006) · 0277-786X/06/$15 · doi: 10.1117/12.666954

content can be so small that even a weakly reactive soil can produce a larger signal. Indeed, the illuminated soil volume is much bigger than that of the metallic part of the mine.

From the above discussion and the number of possible assumptions, it appears that the validity domain of all those assumptions should be clarified. Therefore, we derive general expressions in which the soil and mine contributions are made clear. In those expressions, the incident field is not assumed to be homogeneous on the target. On the contrary, a general multipole expansion is used. In this context, the mine signature is a generalization of the magnetic polarizability tensor and the corresponding dipole field scattered by the mine is obtained by keeping only the first order in our general expressions which allows to assess the accuracy of the dipole model.

The mine contribution is further developed and related to the mine free space signature through a number of TFs characterizing the various soil effects. By computing those TFs, the accuracy of the above mentioned assumptions related to the effects of the soil on the mine signal can immediately be assessed.

Unfortunately, the TFs and other quantities involved in our general expressions can only be computed if the scattering problem is solved. For this numerical techniques are usually required. Such techniques are in general computationally expensive, especially if we want to define the conditions under which the various approximations are valid. This indeed requires to solve the problem for a large parameter set. Therefore, we propose to model a buried mine by a multilayered sphere for which an analytic solution exists.

The paper is organized as follows: Section 2 reviews the multipole expansion. Section 3 discusses the sensor model. Section 4 defines some notations and Section 5 establishes the expression of a contrast response in a general background. Section 6 particularizes this general expression to the case of a mine buried in soil by splitting the total response in a direct coupling and in soil and mine contributions. Section 7 further analyzes the mine response and shows that it can be related to a free space signature through a number of TFs, making explicit the effect of the soil on the mine signature and on the field propagation from the transmit coil to the mine and back to the receive coil. Section 8 uses the analytic solution available for a stratified sphere to compute numerical values for the TFs and other quantities of interest as functions of the relevant parameters such as the soil EM properties or mine depth. A number of classical approximations are discussed in the light of those results. Finally, Section 9 concludes this paper.

2. MULTIPOLE EXPANSION

In a homogeneous sphere which does not contain any sources, the general solution for the fields can be expressed as a spherical multipole expansion [6, Equ. 12 p. 394 and Equ. 11,12 p. 416]*:

$$(\boldsymbol{E},\boldsymbol{H}) = \sum_{pmnd} \alpha^{(\mathrm{d})}_{\mathrm{pmn}} \left(\boldsymbol{E}^{\mathrm{TE,d}}_{\mathrm{pmn}},\boldsymbol{H}^{\mathrm{TE,d}}_{\mathrm{pmn}}\right) + \beta^{(\mathrm{d})}_{\mathrm{pmn}} \left(\boldsymbol{E}^{\mathrm{TM,d}}_{\mathrm{pmn}},\boldsymbol{H}^{\mathrm{TM,d}}_{\mathrm{pmn}}\right) \tag{1}$$

where $\left(\boldsymbol{E}^{\mathrm{TE,d}}_{\mathrm{pmn}},\boldsymbol{H}^{\mathrm{TE,d}}_{\mathrm{pmn}}\right)$ and $\left(\boldsymbol{E}^{\mathrm{TM,d}}_{\mathrm{pmn}},\boldsymbol{H}^{\mathrm{TM,d}}_{\mathrm{pmn}}\right)$ are the fields respectively of a transverse magnetic ($H_{\mathrm{r}} = 0$) and a transverse electric ($E_{\mathrm{r}} = 0$) multipole. The sum is over $p = (o, e)$ (the parity—o for odd, e for even), $m = 0 \rightarrow n$, $n = 0 \rightarrow \infty$ (the multipole order) and $d = (\mathrm{in}, \mathrm{out})$ (the direction of propagation for the multipole—'in' for incoming and 'out' for outgoing). The incoming and outgoing multipoles differ in the solution of the Bessel equation on which they are built. Bessel function of first (j_{n}) and fourth (h_{n}) kind are used respectively for the incoming and outgoing multipoles.

We will denote the multipole expansion (1) by $\left\{\underline{\vec{\alpha}}, \underline{\overleftarrow{\alpha}}, \underline{\vec{\beta}}, \underline{\overleftarrow{\beta}}\right\}$ where $\underline{\alpha}$ and $\underline{\beta}$ are vectors—as indicated by the lower bar—build by the concatenation of the expansion coefficients. The superscript 'd=in' and 'd=out' have been replaced respectively by a left and a right arrow for readability.

To be exact, (1) must include all multipoles orders up to infinity. In practice, the expansion will be truncated at a finite order. We note that the size of the coefficient vectors ($\underline{\alpha}$) and ($\underline{\beta}$) increases quite fast with the order considered as there are $2n + 1$ multipoles for order n. One can easily check that the order zero multipole is null and that for the first order TE multipole, the magnetic field at the origin is along $\hat{\boldsymbol{x}}$, $\hat{\boldsymbol{y}}$ and $\hat{\boldsymbol{z}}$ respectively for,

*The time dependency assumed in this paper is $e^{j\omega t}$ whereas Stratton uses $e^{-j\omega t}$

$\overleftarrow{\alpha}_{e11}$ $\overleftarrow{\alpha}_{o11}$ and $\overleftarrow{\alpha}_{e01}$. Furthermore, this field is homogeneous for $R \ll \lambda$. Therefore, with the normalization defined in [7]:

$$(\overleftarrow{\alpha}_{e11}, \overleftarrow{\alpha}_{o11}, \overleftarrow{\alpha}_{e01}) = \gamma\sqrt{\mu}\boldsymbol{H}(0) \tag{2}$$

where $\boldsymbol{H}(0)$ is the magnetic field at the origin and γ is a normalization factor independent of the frequency and of the medium EM properties. Similarly, one can match the field of a first order outgoing TE multipole with the one of a magnetic dipole at the origin:

$$(\overrightarrow{\alpha}_{e11}, \overrightarrow{\alpha}_{o11}, \overrightarrow{\alpha}_{e01}) = \frac{\sqrt{\mu}}{\gamma}\boldsymbol{m} \tag{3}$$

where m is the magnetic moment of the dipole. Those relations will allow us to match the general results derived in this paper with those found in the literature for dipole approximations.

The above expansion is valid for all frequencies. For a MD, the fields are primarily magnetic and the wavelength in air is much bigger than the dimensions of interest. It is then tempting to define a magnetic scalar potential and to use the corresponding scalar multipole expansion instead of the more complex aforementioned vectorial multipole expansion of the fields. This is however not possible in our problem as a scalar potential can not be defined inside a metallic object. Indeed, inside a metal, the wavelength becomes complex and depends on the skin depth. At the frequencies of interest, the skin depth can become much smaller than the dimension of the object. Nevertheless, there exists a link between the scalar and vectorial expansions. Indeed, at low frequencies and with appropriate normalization, the magnetic field of the vectorial TE multipole and scalar magnetic potential multipole are identical. In other words, at low frequencies, both expansions can be used and the coefficients of the TE (TM) vector expansion can be related to those of the magnetic (electric) scalar potential expansions.

3. SENSOR MODEL

A MD is composed of a transmit (TX) and a receive (RX) coil. In some cases, a single coil is used both for transmission and reception. This configuration can be seen as a degenerated two coils system and the general two-coil model presented in this paper is still valid. As explained below, special care should however be taken if one wants to compute the free space contribution to the received voltage.

Physical coils are complex components. First their winding pattern can be quite complex and the details of manufacture are difficult to obtain in practice. Secondly, accurately predicting the distribution of the current in the wire is a difficult task. Indeed, this distribution is influenced by skin and proximity effects and hence frequency dependent. Furthermore, due to capacitive effects, charges accumulate along the wire. All this makes it difficult to accurately model the fields generated by a real coil. Such an accurate modeling of the coil might be necessary to explain subtle effects such as the effect of water on MD's [8]. In many cases however, it is sufficient to use a simple model in which the coil is considered as a current loop.

The current is then assumed to be concentrated on a one dimensional curve and to remain constant along the coil; effectively neglecting any charge accumulation. Such an ideal coil is then fully characterized by the shape of the loop and the current flowing through it.

Similarly, an accurate modelling of the voltage sensed by the receiver can be related to its transmission characteristics by resorting to reciprocity. Here also, in most cases, good results can be obtained by assuming that the received voltage is proportional to the variation of the magnetic flux flowing across an ideal coil section. The received voltage is then:

$$V_{RX} = j\omega \int_{\mathcal{S}_{loop}} \boldsymbol{B} \cdot \mathrm{d}\boldsymbol{S} = -\int_{\mathcal{C}_{RX}} \boldsymbol{E} \cdot \mathrm{d}\boldsymbol{l} \tag{4}$$

where $\mathcal{C}_{RX}$ is the contour defined by the loop and $\mathcal{S}_{loop}$ is any surface sustained by that contour.

4. NOTATION

In the next sections, we will have to refer to a large number of different fields such as the one generated by the transmit or receive coil in presence and in absence of contrast. Further, as different multipole expansions are needed for a given field, typically one per medium (soil, air, mine etc.), a systematic notation for the fields and their corresponding multipole expansion is introduced to avoid confusion.

All current sources are identified by a label such as 'TX' for a current I_{TX} flowing in the transmit coil. The fields generated by a current source 's' in a given environment 'env' is denoted $\left(\boldsymbol{E}_{\mathrm{s}}^{(\mathrm{env})}, \boldsymbol{H}_{\mathrm{s}}^{(\mathrm{env})}\right)$. For the corresponding multipole expansion $\left\{\underline{\overrightarrow{\alpha}}_{\mathrm{s,r}}^{(\mathrm{env})}, \underline{\overleftarrow{\alpha}}_{\mathrm{s,r}}^{(\mathrm{env})}, \underline{\overrightarrow{\beta}}_{\mathrm{s,r}}^{(\mathrm{env})}, \underline{\overleftarrow{\beta}}_{\mathrm{s,r}}^{(\mathrm{env})}\right\}$, we use an additional subscript to indicate the region ('r') †

5. RESPONSE OF A CONTRAST IN A GENERAL BACKGROUND

This section shows how the voltage induced in the receive coil by the presence of a contrast embedded in a general background can be related to the multipole expansions of the incident and scattered fields. The various multipole expansions involved and the corresponding environment are illustrated in Fig. 1.

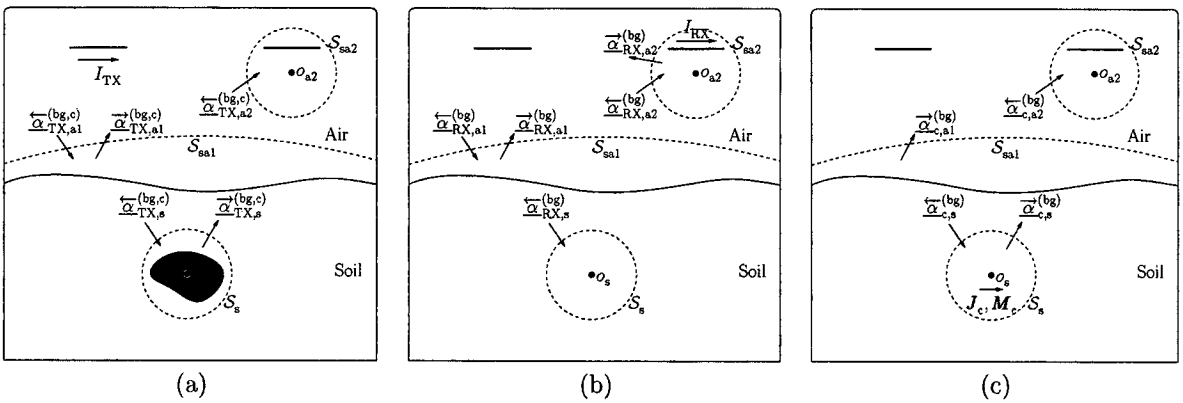

Figure 1. Two states used to apply reciprocity theorem. In (a) current I_{TX} flows in transmit coil and contrast is present. In (b) current I_{RX} flows in receive coil and contrast is absent. In both cases, background is composed of air and soil layer. An additional state used in the derivation is presented in (c) where the contrast is replaced by equivalent currents $(\boldsymbol{J}_{\mathrm{c}}, \boldsymbol{M}_{\mathrm{c}})$. Spheres on which boundary term of the reciprocity theorem is computed are $\mathcal{S}_{\mathrm{s}}$, $\mathcal{S}_{\mathrm{a1}}$ and $\mathcal{S}_{\mathrm{a2}}$. First sphere pertains to the soil and two last to the air medium. Multipole expansions about corresponding sphere centers are identified by $\underline{\alpha}$. Absence of incoming or outgoing wave on drawing indicates a null component which occurs when there is no source and no contrast inside or outside corresponding sphere.

We start by decomposing the total fields in an incident $(\boldsymbol{E}^{\mathrm{inc}}, \boldsymbol{H}^{\mathrm{inc}})$ and a scattered $(\boldsymbol{E}^{\mathrm{scat}}, \boldsymbol{H}^{\mathrm{scat}})$ component. The incident field is the field that would be generated by the transmit coil in absence of the contrast and the scattered field is that additional contribution due to the presence of the contrast. According to the equivalence principle [9, 10], the contrast can be replaced by equivalent currents flowing in the background medium. Those currents $(\boldsymbol{J}_{\mathrm{c}}, \boldsymbol{M}_{\mathrm{c}})$ can be found by solving an integral equation [9, 11–13] and are uniquely determined by the value of the incident fields on the contrast boundary.

With the notation of section 4, the incident and scattered fields are written $\left(\boldsymbol{E}_{\mathrm{TX}}^{(\mathrm{bg})}, \boldsymbol{H}_{\mathrm{TX}}^{(\mathrm{bg})}\right)$ and $\left(\boldsymbol{E}_{\mathrm{c}}^{(\mathrm{bg})}, \boldsymbol{H}_{\mathrm{c}}^{(\mathrm{bg})}\right)$ respectively. Subscript 'TX' indicates a current I_{TX} in the transmit loop and subscript 'c' indicates a current distribution $(\boldsymbol{J}_{\mathrm{c}}, \boldsymbol{M}_{\mathrm{c}})$ on the contrast boundary. Superscript 'bg' indicates that those currents are radiating in an environment which is composed of the background alone.

†Several origins can be used in each region; therefore, rigorously speaking, 'r' also defines the origin of the expansion.

Splitting the received voltage accordingly yields:

$$V_{\mathrm{RX}}^{\mathrm{bg,c}} = V_{\mathrm{RX}}^{\mathrm{bg}} + V_{\mathrm{RX}}^{\mathrm{c}} \tag{5}$$

where each contribution can be related to the corresponding field with (4):

$$V_{\mathrm{RX}}^{\mathrm{bg}} = -\int_{C_{\mathrm{RX}}} \boldsymbol{E}_{\mathrm{TX}}^{(\mathrm{bg})} \cdot \mathrm{d}\boldsymbol{l} \quad V_{\mathrm{RX}}^{\mathrm{c}} = -\int_{C_{\mathrm{RX}}} \boldsymbol{E}_{\mathrm{c}}^{(\mathrm{bg})} \cdot \mathrm{d}\boldsymbol{l} \tag{6}$$

It can be shown, using the reciprocity theorem [7] that the field integral on the receive coil is related to the multipole expansions of an incident and a scattered field:

$$V_{\mathrm{RX}}^{\mathrm{c}} = \frac{j\omega}{I_{\mathrm{RX}}} \left\{ \underline{\overrightarrow{\alpha}}_{\mathrm{c,r}}^{(\mathrm{bg})} \cdot \underline{\overleftarrow{\alpha}}_{\mathrm{RX,r}}^{(\mathrm{bg})} - \underline{\overleftarrow{\alpha}}_{\mathrm{c,r}}^{(\mathrm{bg})} \cdot \underline{\overrightarrow{\alpha}}_{\mathrm{RX,r}}^{(\mathrm{bg})} \right\} \tag{7}$$

where the dot product indicates that there is no coupling between multipoles of different types. The subscript 'RX' indicates that the field to which the multipole expansion corresponds is generated by a current I_{RX} flowing in the receive coil[‡] and the subscript 'r' indicates a homogeneous region such as the soil or the air to which the multipole expansions pertain. This region can be chosen arbitrarily as long as a sphere which separates the transmit coil from the contrast can be drawn in that region. The surface $\mathcal{S}_{\mathrm{s}}$ drawn in Fig. 1 is an example of such a sphere for the soil region. For the air region, $\mathcal{S}_{\mathrm{a1}}$ and $\mathcal{S}_{\mathrm{a2}}$ are two possible spheres. In all cases, the origin of the multipole expansion is at the center of the corresponding sphere and the same origin must be used for the expansion of all fields.

In the above expression, we only included the TE multipoles. In general, a similar contribution must be added for the TM contribution but this contribution can often be neglected for EM induction problems. It is understood that the above expression requires an appropriate normalization of the multipoles.

Another expression of the received voltage can be obtained by noting that according to the definition of the scattered field,

$$\underline{\overrightarrow{\alpha}}_{\mathrm{c,r}}^{(\mathrm{bg})} = \underline{\overrightarrow{\alpha}}_{\mathrm{TX,r}}^{(\mathrm{bg,c})} - \underline{\overrightarrow{\alpha}}_{\mathrm{TX,r}}^{(\mathrm{bg})} \tag{8}$$

and a similar relation for the incoming multipoles. Introducing those expressions for the scattered field into (7) one gets:

$$V_{\mathrm{RX}}^{\mathrm{c}} = \frac{j\omega}{I_{\mathrm{RX}}} \left\{ \underline{\overrightarrow{\alpha}}_{\mathrm{TX,r}}^{(\mathrm{bg,c})} \cdot \underline{\overleftarrow{\alpha}}_{\mathrm{RX,r}}^{(\mathrm{bg})} - \underline{\overleftarrow{\alpha}}_{\mathrm{TX,r}}^{(\mathrm{bg,c})} \cdot \underline{\overrightarrow{\alpha}}_{\mathrm{RX,r}}^{(\mathrm{bg})} \right\} \tag{9}$$

where we have used the relation:

$$\underline{\overrightarrow{\alpha}}_{\mathrm{TX,r}}^{(\mathrm{bg})} \cdot \underline{\overleftarrow{\alpha}}_{\mathrm{RX,r}}^{(\mathrm{bg})} - \underline{\overleftarrow{\alpha}}_{\mathrm{TX,r}}^{(\mathrm{bg})} \cdot \underline{\overrightarrow{\alpha}}_{\mathrm{RX,r}}^{(\mathrm{bg})} = 0 \tag{10}$$

established in [7] by applying reciprocity between fields $\left(\boldsymbol{E}_{\mathrm{TX}}^{(\mathrm{bg})}, \boldsymbol{H}_{\mathrm{TX}}^{(\mathrm{bg})}\right)$ and $\left(\boldsymbol{E}_{\mathrm{RX}}^{(\mathrm{bg})}, \boldsymbol{H}_{\mathrm{RX}}^{(\mathrm{bg})}\right)$. This relation results from the fact that the sources for both states are on the same side of S_{r}.

6. RESPONSE OF A MINE BURIED IN A HOMOGENEOUS SOIL

This section particularizes (5) to the case of a mine buried in a homogeneous soil and will make apparent the mine and background contributions. The mine contribution can readily be computed using (7) and the background contribution can further be developed by noting that the background can be described as a soil volume in free space. In other words, (5) can again be used, this time with the soil as a contrast and free space as the background. This will make apparent the soil contribution and the direct coupling between the transmit and receive coils.

For a mine buried in a homogeneous soil, (5) yields

$$V_{\mathrm{RX}}^{\mathrm{as,m}} = V_{\mathrm{RX}}^{\mathrm{as}} + V_{\mathrm{RX}}^{\mathrm{m}} \tag{11}$$

[‡]This current does not exist physically but appears in one of the states defined to apply the reciprocity theorem.

where the superscripts 'as' and 'm' stand respectively for the air-soil background and the mine. According to (7) and (9),

$$V_{\mathrm{RX}}^{\mathrm{m}} = \frac{j\omega}{I_{\mathrm{RX}}} \left\{ \underline{\overrightarrow{\alpha}}_{\mathrm{TX,a}}^{(\mathrm{as,m})} \cdot \underline{\overleftarrow{\alpha}}_{\mathrm{RX,a}}^{(\mathrm{as})} - \underline{\overleftarrow{\alpha}}_{\mathrm{TX,a}}^{(\mathrm{as,m})} \cdot \underline{\overrightarrow{\alpha}}_{\mathrm{RX,a}}^{(\mathrm{as})} \right\} \tag{12a}$$

$$= \frac{j\omega}{I_{\mathrm{RX}}} \underline{\overrightarrow{\alpha}}_{\mathrm{c,a}}^{(\mathrm{as})} \cdot \underline{\overleftarrow{\alpha}}_{\mathrm{RX,a}}^{(\mathrm{as})} \tag{12b}$$

for the multipole expansion pertaining to the air region (subscript 'a') and:

$$V_{\mathrm{RX}}^{\mathrm{m}} = \frac{j\omega}{I_{\mathrm{RX}}} \underline{\overrightarrow{\alpha}}_{\mathrm{TX,s}}^{(\mathrm{as,m})} \cdot \underline{\overleftarrow{\alpha}}_{\mathrm{RX,s}}^{(\mathrm{as})} \tag{13a}$$

$$= \frac{j\omega}{I_{\mathrm{RX}}} \underline{\overrightarrow{\alpha}}_{\mathrm{c}}^{(\mathrm{as})} \cdot \underline{\overleftarrow{\alpha}}_{\mathrm{RX,s}}^{(\mathrm{as})} \tag{13b}$$

for the multipole expansion pertaining to the soil region (subscript 's'). The simplifications stem from the fact that the origin is chosen inside the contrast and therefore $\underline{\overrightarrow{\alpha}}_{\mathrm{RX,s}}^{(\mathrm{as})} = 0$ and $\underline{\overleftarrow{\alpha}}_{\mathrm{m,a}}^{(\mathrm{as})} = 0$.

By limiting the expansion to the first order and using (2) and (3), one recovers the classical dipole approximation [1, Equ. 2.21 p. 23][2, 3]:

$$V_{\mathrm{RX}}^{\mathrm{m}} = \frac{j\omega\mu}{I_{\mathrm{RX}}} \boldsymbol{m}_{\mathrm{m}}^{\mathrm{as}} \cdot \boldsymbol{H}_{\mathrm{RX}}^{(\mathrm{as})} \tag{14}$$

where $\boldsymbol{m}_{\mathrm{m}}^{\mathrm{as}}$ is the magnetic dipole moment of the mine and $\boldsymbol{H}_{\mathrm{RX}}^{(\mathrm{as})}$ is the magnetic field produced by the receive coil at the mine location. The superscripts emphasize the fact that both quantities are influenced by the presence of the air-soil background.

We again use (5) to further split the air-soil background contribution in a soil and free space contribution by considering the air-soil background as a soil contrast in a free space background, which yields:

$$V_{\mathrm{RX}}^{\mathrm{as,m}} = V_{\mathrm{RX}}^{\mathrm{fs}} + V_{\mathrm{RX}}^{\mathrm{s}} + V_{\mathrm{RX}}^{\mathrm{m}} \tag{15}$$

where the superscripts 'fs' and 's' stand respectively for free space background and soil. The free space, soil and mine contributions to the received voltage clearly appear from the above expression.

The free space contribution is the free space direct coupling between the transmit and receive coils. It is a characteristic of the sensor and could be computed from the coils' shape and relative position. We note however that when the TX and RX coils are close to each other, the direct coupling is very sensitive to small details of the coil geometry. The worst case appears when a single coil is used for transmission and reception. The simple coil model used here can then clearly not be used because it would lead to an infinite value for $V_{\mathrm{RX}}^{\mathrm{fs}}$. This is related to the fact that the self inductance of an infinitely thin wire is infinite. To get a reasonable estimate of $V_{\mathrm{RX}}^{\mathrm{fs}}$ one has at least to account for the finite radius of the wire. Fortunately, computing $V_{\mathrm{RX}}^{\mathrm{fs}}$ is usually not required as it can easily be measured. Furthermore, it has little effect on sensor performances, as this direct coupling is measured during the sensor calibration and then canceled by the electronics.

According to (7) and (9), the soil contribution can only be computed in the air region and can be expressed as follows:

$$V_{\mathrm{RX}}^{\mathrm{s}} = \frac{j\omega}{I_{\mathrm{RX}}} \underline{\overrightarrow{\alpha}}_{\mathrm{TX,a}}^{(\mathrm{fs,s})} \cdot \underline{\overleftarrow{\alpha}}_{\mathrm{RX,a}}^{(\mathrm{fs})} \tag{16a}$$

$$V_{\mathrm{RX}}^{\mathrm{s}} = \frac{j\omega}{I_{\mathrm{RX}}} \underline{\overrightarrow{\alpha}}_{\mathrm{s,a}}^{(\mathrm{fs})} \cdot \underline{\overleftarrow{\alpha}}_{\mathrm{RX,a}}^{(\mathrm{fs})} \tag{16b}$$

where we made use of $\underline{\overrightarrow{\alpha}}_{\mathrm{RX,a}}^{(\mathrm{fs})} = 0$ and $\underline{\overleftarrow{\alpha}}_{\mathrm{s,a}}^{(\mathrm{fs})} = 0$ which stems from the fact that the origin of the multipole expansions is chosen inside the soil.

7. ANALYSIS OF THE MINE RESPONSE

This section defines the mine signature and a number of TFs allowing to account for the effect of the soil on that signature and on the transmission from the transmit coil to the mine and back to the receive coil.

According to the equivalence principle, the mine can be replaced by a distribution of currents flowing in the soil on the mine boundary. Those currents can be found as a function of the incident fields at the mine boundary by solving an integral equation [12]. The mine is assumed to be buried below the soil surface and the soil is assumed to be homogeneous around the mine. The incident and scattered fields can then be expressed as incoming and outgoing multipole expansions respectively. For linear media, the relation between those expansions can be written:

$$\underline{\vec{\alpha}}_{\mathrm{c,s}}^{(\mathrm{as})} = \underline{\underline{M}}_{\mathrm{m}}^{(\mathrm{as})} \underline{\overleftarrow{\alpha}}_{\mathrm{TX,s}}^{(\mathrm{as})} \tag{17}$$

where the subscript 's' indicates the soil medium and $\underline{\underline{M}}_{\mathrm{m}}^{\mathrm{as}}$ is the target signature of the mine as indicated by the subscript 'm'. The superscript 'as' indicates that this signature is a function of the environment; here the background composed of an air and a soil layer.

In the above expression, we assume that the incident field exclusively contains TE multipoles but the expression remains valid in the general case if the TE and TM multipoles are concatenated. In the later case, the size of the target signature matrix is multiplied by four.

According to (2), (3), limiting the multipole expansion to first order yields:

$$\boldsymbol{m}_{\mathrm{m}} = \gamma^2 \underline{\underline{M}}_{\mathrm{m}}^{(\mathrm{as})} \boldsymbol{H}_{\mathrm{inc}} \tag{18}$$

where $\boldsymbol{m}_{\mathrm{m}}$ is the magnetic dipole moment of the mine and $\boldsymbol{H}_{\mathrm{inc}}$ is the magnetic field incident on the mine. This expression is similar to [1, Equ. 2.20 p. 23] which shows that the first order approximation of the mine signature is proportional to the magnetic polarizability tensor.

In a similar manner, we define the signature of the mine in an infinite soil and in free space as $\underline{\underline{M}}_{\mathrm{m}}^{(\mathrm{s})}$ and $\underline{\underline{M}}_{\mathrm{m}}^{(\mathrm{fs})}$. We then define TFs linking those signatures to each other:

$$\underline{\underline{M}}_{\mathrm{m}}^{(\mathrm{as})} = \underline{\underline{H}}_{\mathrm{int}} \underline{\underline{M}}_{\mathrm{m}}^{(\mathrm{s})} \tag{19}$$

$$\underline{\underline{M}}_{\mathrm{m}}^{(\mathrm{s})} = \underline{\underline{H}}_{\mathrm{soil}} \underline{\underline{M}}_{\mathrm{m}}^{(\mathrm{fs})} \tag{20}$$

where $\underline{\underline{H}}_{\mathrm{int}}$ links the signature in the multilayered background to its full space soil counterpart and represents the effect of the air-soil interface. $\underline{\underline{H}}_{\mathrm{soil}}$ links the signature in a fullspace soil to its free space counterpart and represents the effect of the soil.

To characterize the effect of the soil on the field transmission from the transmit coil to the target and back to the receive coil, we define the transmit and receive TFs by:

$$\underline{\overleftarrow{\alpha}}_{\mathrm{TX,s}}^{\mathrm{as}} = \underline{\underline{H}}_{\mathrm{TX}} \underline{\overleftarrow{\alpha}}_{\mathrm{TX,s}}^{\mathrm{fs}} \tag{21}$$

$$\underline{\overleftarrow{\alpha}}_{\mathrm{RX,s}}^{\mathrm{as}} = \underline{\underline{H}}_{\mathrm{RX}} \underline{\overleftarrow{\alpha}}_{\mathrm{RX,s}}^{\mathrm{fs}} \tag{22}$$

we now rewrite (13b) using the matrix product instead of the dot product:

$$V_{\mathrm{RX}}^{\mathrm{m}} = \frac{j\omega}{I_{\mathrm{RX}}} \left(\underline{\vec{\alpha}}_{\mathrm{c,s}}^{(\mathrm{as})} \right)' \underline{\overleftarrow{\alpha}}_{\mathrm{RX,s}}^{(\mathrm{as})} \tag{23}$$

in which we introduce (17),(19),(20), (21) and (22) to get:

$$V_{\mathrm{RX}}^{\mathrm{m}} = \frac{j\omega}{I_{\mathrm{RX}}} \left(\underline{\overleftarrow{\alpha}}_{\mathrm{TX,s}}^{(\mathrm{fs})} \right)' \left(\underline{\underline{H}}_{\mathrm{TX}} \right)' \underline{\underline{H}}_{\mathrm{int}} \underline{\underline{H}}_{\mathrm{soil}} \underline{\underline{M}}_{\mathrm{m}}^{(\mathrm{fs})} \underline{\underline{H}}_{\mathrm{RX}} \underline{\overleftarrow{\alpha}}_{\mathrm{RX,s}}^{(\mathrm{fs})} \tag{24}$$

which clearly shows the various effects of the soil on the target response. When one effect is not significant, the corresponding TF will tend to unity. For example, if $\underline{\underline{H}}_{\mathrm{int}}$ is close to unity, the air soil interface has no

significant effect and the target signature in the soil can be approximated by its soil fullspace counterpart. This assumption was used in [3]. If furthermore, $\underline{\underline{H}}_{\text{soil}}$ is close to unity, the in soil signature can be approximated by its free-space counterpart. This is very useful in practice because the target can be fully characterized by its free-space signature that can be measured with an appropriate setup. If furthermore $\underline{\underline{H}}_{\text{TX}}$ and $\underline{\underline{H}}_{\text{RX}}$ are close to unity, the target response can be computed by completely neglecting the soil. We will then say that the soil is transparent. In this case, the computation of the target response is much simpler because all that is required is the free space radiation pattern of the transmit and receive coils and the free space signature of the target. The fact that the soil is transparent does however not imply that it has no effect at all. On the contrary, according to (15), the soil still has a direct contribution to the received voltage and the target of interest can be so small that the response of the large illuminated soil volume dominates the response of the target even if the soil does not influence the mine response.

8. NUMERICAL RESULTS

In the previous sections, we have shown how the soil and mine responses, the mine signature as well as a number of TFs appearing in (24) and characterizing the importance of the various soil effects can be computed once the multipole expansions of the relevant fields are known. To compute those multipole expansions one must solve the scattering problem, and this requires in general the use of numerical techniques. However, there exists particular configurations for which an analytic solution can be used to compute the multipole expansions.

One such configuration is a layered sphere, for which the analytic solution yields the coefficients of all the required multipole expansions [14] as a function of the multipole expansion of the excitation field and the EM properties of the various layers. The layered sphere has been used for a number of problems such as modeling the human head [15] or a stratified lens [16,17].

Note that due to the spherical shape of the interfaces, no cross coupling exists between the multipoles. In other words, the problem can be solved independently for each multipole appearing in the expansion of the source. This implies that all the matrices appearing in (24) become diagonal, which greatly reduces the number of parameters to consider.

Figure 2 shows the mapping of the physical problem to a layered sphere. The outer layer represents the air and the next layer the soil. Two additional layers are used to model the mine. The inner sphere represents the mine metallic content and the intermediate layer represents the explosive. The origin for all the multipole expansions is at the common center of the spheres. The radii for the various spheres are denoted R_{metal}, $R_{\text{explosive}}$ and R_{soil}.

A frequency of 5kHz which is typical for MD has been chosen. The EM properties are $\epsilon_{\text{metal}} = \epsilon_0$, $\mu_{\text{metal}} = \mu_0$, $\sigma_{\text{metal}} = 3.54\ 10^7$ S/m; $\epsilon_{\text{explosive}} = 3\epsilon_0$, $\mu_{\text{explosive}} = \mu_0$, $\sigma_{\text{explosive}} = 0$ and $\epsilon_{\text{soil}} = 10\epsilon_0$, $\sigma_{\text{soil}} = 0$ respectively for the metal, explosive and soil spheres. The only EM property that is not fixed is the soil magnetic permeabilityμ_{soil}. This parameter will be varied in the simulations in the range 1 to 1.5 μ_0. The upper limit is quite conservative and most soils of interest will have relative permeabilities much lower than 1.5. A typical value for laterite, known to significantly affect MDs, is 1.002.

Actually, we also varied the soil conductivity in the range 0 to 5 S/m but there was no visible change in the plots presented. We note that a conductivity of 5 S/m is 'likely higher than the conductivity of sea water saturated soil' [2]. There might however exist soils containing ferrous oxides for which the resulting conductivity is much higher. Those cases are however very specific, and in most cases of interest, the soil conductivity does not play any significant role.

The conductivity chosen for the metal is characteristic of aluminum. The electrical permittivity of the soil can vary significantly as function of its water content but this is not an issue because the electrical permittivity has no significant influence on a MD as can easily be verified by varying ϵ in the simulations.

The transmit and receive coils are modeled by circular loops in horizontal planes. The radius of the transmit loop is a_{TX} and its center is at $(0, 0, z_{\text{TX}})$. In spherical coordinates, the transmit loop is characterized by $R = R_{\text{TX}}$ and $\theta = \theta_{\text{TX}}$. The reception loop is similarly characterized by a_{RX}, R_{RX} and $\theta = \theta_{\text{RX}}$. For the coils, we have used parameters representative of the Schiebel AN19/2 MD: $a_{\text{TX}} = 12$cm, $a_{\text{RX}} = 9.025$cm and both coils are in the same plane $z_{\text{TX}} = z_{\text{RX}} = z_{\text{coil}}$. The common height of the coils is $h = z_{\text{coil}} - R_{\text{soil}}$.

With the chosen coils geometry, the problem exhibits a symmetry of rotation around the z-axis. This ensures that only multipoles with $m = 0$ needs to be considered, effectively reducing the number of coefficients to consider. Furthermore, the required multipole expansion of the excitation field can easily be computed as shown in [7].

8.1. An example

To illustrate the effect of the various layers, we have computed the fields for $R_{\text{metal}} = 2\text{cm}$, $R_{\text{explosive}} = 4\text{cm}$, $R_{\text{soil}} = 10\text{cm}$, $\mu_{\text{soil}} = 5\mu_0$ and $h = 0\text{cm}$. The magnetic permeability used for the soil layer is much higher than what is expected for real soils. Such a high value was chosen to make the effect of the magnetic contrast more visible.

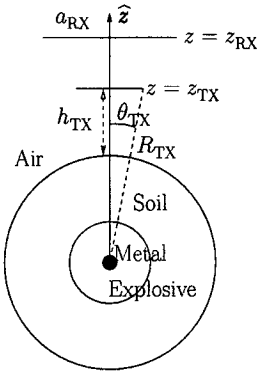

Figure 2. Layered sphere model used for mine buried the soil.

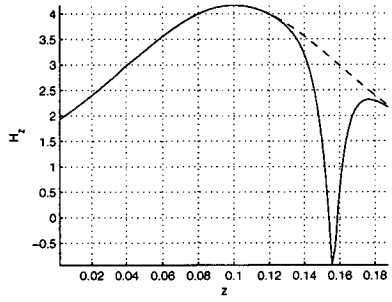

Figure 3. Magnetic field on the axis of a circular loop located at $z_{\text{loop}} = 15\text{cm}$. Analytic expression (– –) and multipole expansion to order 20 (—).

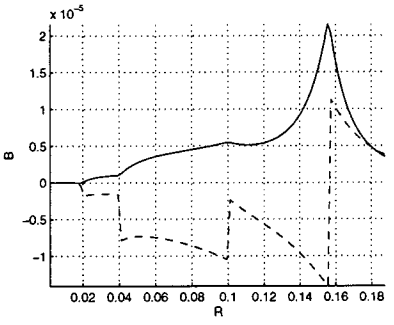

Figure 4. Real part of radial (—) and transverse (– –) component of magnetic induction on a radial line for $\theta = \pi/4$, $R_{\text{metal}} = 2\text{cm}$, $R_{\text{explosive}} = 4\text{cm}$, $R_{\text{soil}} = 10\text{cm}$, $\mu_{\text{soil}} = 5\mu_0$ and $h = 0\text{cm}$.

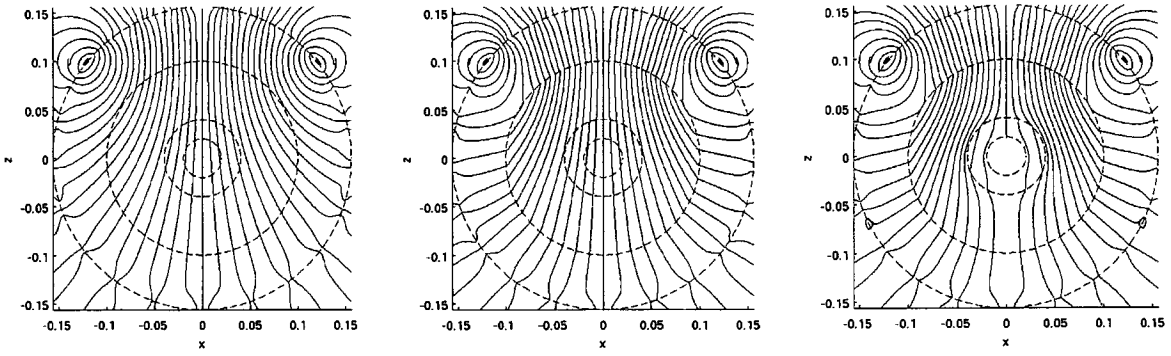

Figure 5. Field lines of real part of $\boldsymbol{H}$ for excitation field (a) and total field in presence of the soil alone (b) and in presence of soil and mine (c). Parameters are $R_{\text{metal}} = 2\text{cm}$, $R_{\text{explosive}} = 4\text{cm}$, $R_{\text{soil}} = 10\text{cm}$, $\mu_{\text{soil}} = 5\mu_0$ and $h = 0\text{cm}$.

The resulting field lines of the magnetic field are illustrated in Fig. 5 where a cut in the xz-plane is shown. By symmetry the result would be identical for any other plane containing the z-axis. The inner circles are the interfaces between the different media and the outer circle is the cut in the sphere containing the transmit loop. The radius of this sphere is $R_{\text{TX}} = \sqrt{a_{\text{TX}}^2 + Z_{\text{TX}}^2} = 15.62\text{cm}$. The coil cuts the xz-plane ar two points which are

drawn as dots. The fields are complex and therefore, when the real and imaginary component of the fields are not parallel, the field lines are changing with time. The field lines presented are those for the real part of the fields which correspond to $t = 0$.

In Fig. 5a, the excitation field is shown. This is the field produced by the excitation coil in free space. Figures 5b and 5c show respectively the field in presence of the soil alone and in presence of the soil and the mine. As expected, the effect of the magnetic layer is to deform the field lines to minimize the in air path and the currents induced in the metal keep the magnetic field outside the inner sphere.

The artifacts in the neighborhood of the sphere containing the transmit coil are due to the fact that for the excitation field, two multipole expansions are required, one inside and another outside that sphere. When approaching the excitation sphere, the convergence becomes very slow and a high order expansion is required. This phenomenon is further illustrated on Fig. 3 where a multipole expansion of order 20 is compared to the analytic solution on the z-axis. The multipole expansion is quite accurate except in the neighborhood of the excitation sphere. This plot also validates our expression for the coefficients of the excitation field multipole expansion.

Finally in Fig. 4 the magnetic induction on a radial line for $\theta = \pi/4$ is plotted. The magnetic field decreases fast to zero inside the metal, highlighting the skin effect. The radial component of the magnetic induction, which is normal to the interface, is continuous across the interfaces as required to satisfy the boundary conditions. This and similar verifications for the fields $\boldsymbol{H}$, $\boldsymbol{E}$ and $\boldsymbol{D}$ yield a validation of our implementation of the multilayered sphere solution.

8.2. Dipole approximation

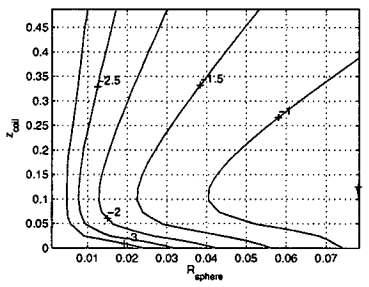

Figure 6. Error of dipole approximation $\log\left|\frac{V^1_{\mathrm{RX}} - V^{20}_{\mathrm{RX}}}{V^{20}_{\mathrm{RX}}}\right|$ for metallic sphere as function of sphere radius and coil height

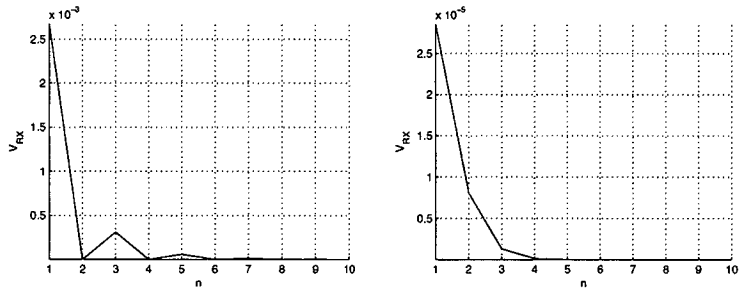

(a) (b)

Figure 7. Contribution of multipoles to response of metallic sphere of radius 7 cm for coil height of 0 cm (a) and 20 cm (b) as function of their order.

An common assumption [1, 3] is to consider that the field radiated by the mine as seen by the receiver can be approximated by the field of a dipole. The magnetic moment of that dipole is furthermore assumed to be linearly related to the incident field at a reference point on the mine. The mine is then fully characterized by its magnetic polarizability tensor.

In our framework this approximation appears as the first order approximation of the received voltage V^1_{RX}. In Fig. 6 we have compared this first order approximation to the result obtained with an multipole expansion of order 20 (V^{20}_{RX})for a metallic sphere. The error is shown as function of the radius of the sphere and the height of the coil above the sphere center. A logarithmic scale is used and therefore the contour line labeled '-2' corresponds to a relative error of one percent.

For spheres smaller than 1 cm, the dipole approximation yield a good accuracy but the error can significantly exceed one percent for bigger spheres which might be representative of mines with large metal content or even mines with a low metal content scattered in the mine volume. We note that in our current implementation, the

sphere is constrained to be located on the axis of the coil where the field is the most homogeneous. Higher errors are expected for spheres located off-axis, especially close to the coil.

It might look surprising that when the height of the coil is increased, the error first increases. This can be explained by the fact that when the sphere and coil center are co-located, the xy-plane is a plane of symmetry and therefore the order 2 multipole does not contribute to the field expansion. Therefore, the error is mainly due to the order 3 multipole whereas when the coil is raised, the order two multipole starts to contribute significantly to the error as illustrated in Fig. 7.

8.3. Soil response

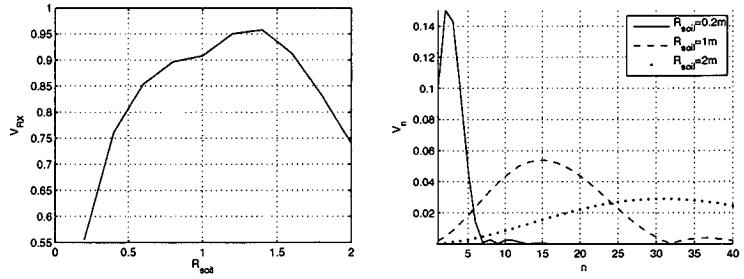

(a) (b)

Figure 8. Soil response as function of radius of sphere representing soil for magnetic soil with $\mu_{\text{soil}} = 1.5\mu_0$. Coil is located 1 cm above the ground. In (a) total response for a multipole expansion of order 40 normalized by corresponding half-space response. In (b) contribution of multipoles as function of their order.

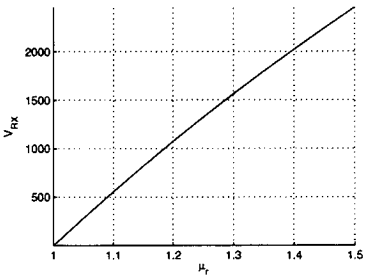

Figure 9. Ratio of the soil to reference metallic sphere response for $z_{\text{coil}} =$ 1cm. Reference sphere has radius of 5mm and is located on axis of coils at 10 cm from coil plane.

In our framework, the soil is modelled as a spherical layer. This obviously is not quite representative of a real air-soil interface especially for a small radius of the sphere layer. When the radius is increased, the part of the interface in the footprint of the detector can be made arbitrarily flat. We therefore expect the soil response to converge to the response of a half space with the same EM properties when the radius of the soil sphere is increased.

This is illustrated in Fig. 8a where the soil response is shown as function of the radius of the soil sphere for a purely magnetic soil $\mu_{\text{soil}} = 1.5\mu_0$. The coil is 1 cm above the ground and the response is normalized with the half-space response computed by [3, Equ. 10 and 11]. The curve does not reach one as expected because the order of the expansion had to be limited to 40 for numerical reasons and as shown in Fig. 8b, the contribution of higher order multipoles increases with the radius of the soil sphere. Truncating the expansion at order 40 yields a significant underestimation of the response for spheres bigger than 1 m.

A better normalization could be implemented to reduce numerical problems appearing with high order expansions. The current implementation is however sufficient for the purpose of this paper because the soil radius is limited by the mine depth considered. Indeed, the current implementation constraints the spheres to have a common center. The radius of the soil sphere is then equal to the mine depth.

In the next section, a radius of 10 cm will be used for the soil sphere and the detector will be put 1 cm above that sphere. From Fig. 8 it appears that this will yield an underestimation of the soil response by a factor bigger than 10. Even so, Fig. 9 shows that the soil response can be significantly bigger than that of a reference metallic sphere. The reference sphere has a radius of 5mm and is located on the axis of the coils at 10 cm from the coil plane. We note that the response of the reference sphere in free space can easily be computed using our model. The result of the first order approximation should be identical to Equ. 7 and 8 in [3]. We have checked that both results are indeed identical, yielding an additional validation of our implementation.

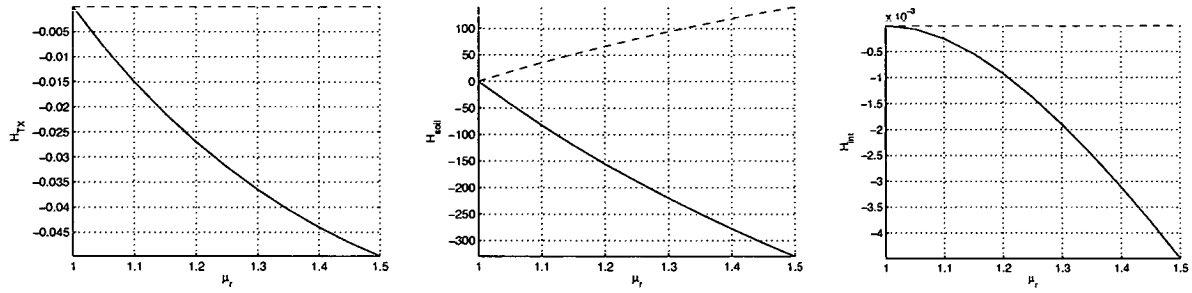

Figure 10. TFs for $R_{\text{metal}} = 5\text{mm}$, $R_{\text{explosive}} = 5\text{cm}$, $R_{\text{soil}} = 10\text{cm}$ and $h = 1\text{cm}$ as function of the soil magnetic permeability. Real part minus one (—) and imaginary part (– –) of H_{TX} (a), H_{soil} (b) and H_{int} (c).

8.4. Transfer functions

Figure 10 shows the various TFs appearing in (23) for a typical configuration characterized by $R_{\text{metal}} = 5\text{mm}$, $R_{\text{explosive}} = 5\text{cm}$, $R_{\text{soil}} = 10\text{cm}$ and $h = 1\text{cm}$ as function of the soil magnetic permeability. The TF H_{RX} is not presented but it is similar to H_{TX}.

One sees that the soil has a moderate effect on the field propagation (Fig. 10a) and that the air-soil interface only has a marginal effect on the mine signature (Fig. 10c). Hence, for the configuration considered the approximation made in [3] is validated. The effect of the air-soil interface is further investigated in Fig. 12 where H_{int} is

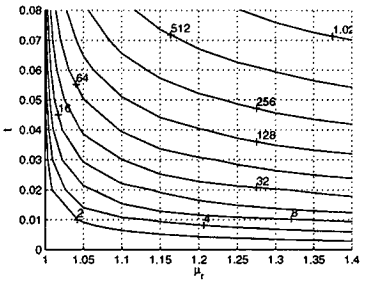

Figure 11. TF H_{soil} as function of soil magnetic permeability and thickness of explosive layer.

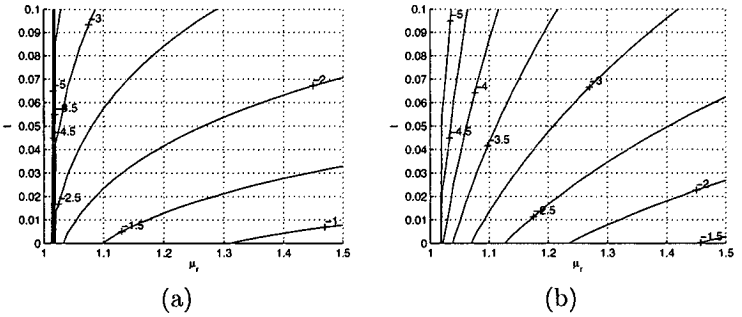

Figure 12. TF $\log\{1 - |H_{\text{int}}|\}$ as function of soil magnetic permeability and thickness of soil layer for $R_{\text{metal}} = 5\text{mm}$ and $R_{\text{explosive}} = 5\text{cm}$ (a) and for $R_{\text{metal}} = 5\text{cm}$ and no explosive layer (b).

shown as function of the thickness of the soil layer and the soil magnetic permeability for two mine configurations. In Fig. 12a small metal volume and an explosive layer is considered, while in Fig. 12b the explosive has been replaced by metal. The TF H_{int} represents the effect of the multiple reflections between the mine-soil and soil-air interfaces. This effect is expected to be most significant when the reflections are important. The reflection at the air-soil interface is always weak because the soil is weakly magnetic. On the contrary, the reflection on a good conductor is very high. Therefore, the effect of the interface is expected to be bigger for the second case where the mine contains a large metallic sphere. This is confirmed on the plots presented. Due to the size of the metallic sphere used in 12b, we expect this case to be an upper bound of the effect of the air-soil interface.

We now turn our attention to the last TF which characterizes the effect of the soil on the mine signature. As seen on Fig. 10b the soil can change the mine signature by a factor exceeding 300 for a soil relative permittivity of 1.5. Such a high value for H_{soil}, which might look surprising, is a manifestation of the void effect. Indeed, as shown on Fig. 9a, a 10 cm soil sphere can yield a much bigger response than the reference metallic sphere

which is identical to the metal content of the mine considered. Therefore for a mine radius of 5 cm, the removal of the corresponding soil volume can have a significant effect on the total response. This shows the importance of incorporating the explosive layer in the model.

To further analyze the effect of the explosive layer, we have plotted in Fig. 11 the TF H_{soil} as function of the thickness of the explosive shell and the soil magnetic permeability.

For many configurations, the void effect is quite significant. The fact that the TF H_{soil} significantly differs from 1 seems to indicate that the soil can not be considered as transparent because it significantly modifies the mine response. We however believe that this pitfall can be avoided by modifying the definition of the mine response. The objective of this modification is to make the void contribution to the total response explicit. For this, the mine response should be defined as the difference between the total response and the response of the soil in which the mine volume has been replaced by air. This last response can then be expressed as the sum of a soil and void contribution. With such a decomposition, we expect the TF H_{soil} to become much closer to one. Only if this is confirmed, can the soil be said to be transparent in the sense that the total response is the sum of the soil, void and mine response and that the mine response is not influenced by the soil. This point will be the subject of future research.

9. CONCLUSION AND PERSPECTIVES

We have shown how the soil and mine contribution to the total response of a MD can be related to the multipole expansions of the relevant fields. The mine response has further been related to a free space signature, which is uniquely related to the mine, through a number of TFs which characterize:

- the field propagation from the transmit coil to the mine and back to the reception coil H_{TX} and H_{RX}
- the effect of the soil on the mine signature H_{soil}
- the effect of the air-soil interface on the mine signature H_{int}

The proposed framework is quite general as it only requires that a spherical shell in which the medium is homogeneous can be defined around the receive coil or the mine volume.

We have then applied this framework to a configuration in which a mine buried in soil is modeled by a layered sphere. For such a configuration, an analytic solution is available and was used to compute the soil and mine response as well as the mine signature and the various TFs.

Although the model used is a rough representation of reality, especially when it comes to the shape of the soil volume, it provided very interesting results.

First, it confirmed that even when the soil can be considered as transparent, the soil contribution to the total response can dominate the mine contribution. Secondly, the TFs that we have defined allow to test whether the soil can be considered transparent or not. For the soil to be transparent, all TFs should be close to one. We have shown that in most cases, neither the field propagation (H_{TX}) nor the air-soil interface (H_{int}) has a significant effect on the mine response. However, as surprisingly as it may look, the soil (H_{soil}) can significantly influence the mine signature, even for weakly magnetic soil. This phenomenon was related to the void effect and we therefore discussed the possibility to modify the definition of the mine response to make the void contribution explicit. It is expected that if the void contribution is separated from the mine response, the TF H_{soil} will become close to one. As a consequence, the soil could be considered as transparent as it does not modify the mine response but this require an additional void contribution to be considered. This point will be the subject of future research.

Thirdly the model allowed us to compute the error introduced by the often used dipole approximation. With this approximation, the mine is fully characterized by its magnetic polarizability tensor. The mine signature we have defined is a generalization of this magnetic polarizability tensor which is recovered if the multipole expansions are truncated at first order. We have shown that the dipole approximation is accurate for mines containing a small localized metal volume but that it can introduce a significant error for mines with large metal content or even mines with a low metal content scattered inside the mine volume. For such cases, we have shown that the accuracy can be significantly increased by considering the second and third order multipoles.

We are considering a number of improvements to the model to better take into account the air-soil interface such as the use of non-concentric spheres [18] or expressions for the multipole reflection on a plane interface [19] or, for purely magnetic soils, the simpler image theory [6, p. 194]. We finally note that although the results presented in this paper allows to better understand the influence of the soil on the response of a MD they can not be used as such to quantify the effect on the detector sensitivity. For this it is required to expand the model in order to take into account the MD processing, including soil compensation.

ACKNOWLEDGMENTS

The Author acknowledges the Belgian Ministry of Defence which has funded this work. He is also grateful to I. van den Bosch for his useful comments and suggestions.

REFERENCES

1. C. E. Baum, *Detection and Identification of Visually Obscured Targets*, Taylor and Francis, 1998.
2. Y. Das, "A preliminary investigation of the effects of soil electromagnetic properties on metal detectors," in *Proc. SPIE Conference on Detection and Remediation Technologies for Mines and Mine-like Targets IX, 5415*, pp. 677–690, (Orlando, FL, USA), April 2004.
3. Y. Das, "Electromagnetic induction response of a target buried in conductive and magnetic soil," in *Proc. SPIE Conference on Detection and Remediation Technologies for Mines and Mine-like Targets X, 5794*, pp. 263–274, (Orlando, FL, USA), June 2005.
4. C. Bruschini, *A Multidisciplinary Analysis of Frequency Domain Metal Detectors for Humanitarian Demining*, Vije Universiteit Brussel, Belgium, 2002. Ph.D. dissertation.
5. J. C. Cook and S. L. Carts, "Magnetic effects and properties of typical topsoils," *Journal of geophysical research* **67**, pp. 815–828, February 1962.
6. J. Stratton, *Electromagnetic theory*, McGraw-Hill Book Company, 1941.
7. P. Druyts, C. Craeye, Y. Das, and M. Acheroy, "Applying reciprocity to spherical multipoles," *In preparation* .
8. Y. Das, J. Toews, D. Rutkay, and J. McFee, "Effect of water on canadian forces' an19/2 mine detector," *Defence Research Establishment Suffield* , October 1996.
9. R. F. Harrington, "Boundary integral formulations for homogeneous material bodies," *Journal of Electromagnetic Waves and Applications* **3**, pp. 1–15, January 1989.
10. R. F. Harrington, *Time-Harmonic Electromagnetic Fields*, IEEE, 1961.
11. N. Morita, N. Kumagai, and J. R. Mautz, *Integral Equation Methods for Electromagnetics*, Artech House, Boston, 1990.
12. A. F. Peterson, S. L. Ray, and R. Mittra, *Computational Methods for Electromagnetics*, IEEE/OUP Series on Electromagnetic Wave Theory, IEEE Press, New York, 1998.
13. W. C. Chew, J.-M. Jin, E. Michielssen, and J. Song, *Fast and Efficient Algorithms in Computational Electromagnetics*, Artech House, Norwood, MA 02062, 2001.
14. W. C. Chew, *Waves and Fields in Inhomogeneous Media*, Van Nostrand Reinhold, 1990.
15. K. S. Nikita, G. S. Stamatakos, N. K. Uzunoglu, and A. Karafotias, "Analysis of the interaction between a layered spherical human head model and a finite-length dipole," *IEEE Transactions on Microwave Theory and Techniques* **48**, pp. 2003–2013, November 2000.
16. J. R. Sanford, "Scattering by spherically stratified microwave lens antennas," *IEEE Transactions on Antennas and Propagation* **42**, pp. 690–698, May 1994.
17. H. Mieras, "Radiation pattern computation of a spherical lens using mie series," *IEEE Transactions on Antennas and Propagation* **30**, pp. 1221–1224, November 1982.
18. B. Stout, C. Andraud, S. Stout, and J. Lafait, "Absorption in multiple-scattering systems of coated spheres," *Journal of Optical Society of America* **20**, pp. 1050–1059, June 2003.
19. E. Fucile, F. Borghese, P. Denti, R. Saija, and O. I. Sindoni, "General reflection rule for electromagnetic multipole fields on a plane interface," *IEEE Transactions on Antennas and Propagation* **45**, pp. 868–875, May 1997.